A Platinum Open Access Journal for Organic Chemistry

Paper

Free to Authors and Readers

DOAJ Seal

Arkivoc **2026**, part __, 0-0

to be inserted by editorial office

Synthesis of a π-fused acenaphthylene-imidazole structure and its evaluation as a chromophore for a dye-sensitized solar cell

Gabriela Malta, J. Carlos Lima, A. Jorge Parola,* and Paula S. Branco*

LAQV@REQUIMTE, Chemistry Department of NOVA School of Science and Technology, NOVA FCT, NOVA Lisbon University, Campus de Caparica, 2829-516 Caparica, Portugal

Email: paula.branco@fct.unl.pt ajp@fct.unl.pt

Received mm-dd-yyyy **Accepted** mm-dd-yyyy **Published on line** mm-dd-yyyy

Dates to be inserted by editorial office

Abstract

The synthesis for the first time of a π-fused acenaphthylene-imidazole structure as 7*H*-acenaphtho[1,2-*d*]imidazole (**5**) is here presented alongside its evaluation in dye-sensitized solar cells (DSSCs). The photophysical properties of the compound were characterized using UV-Vis absorption and emission spectroscopy. Revealing an absorption and emission maxima at 390 nm and 570 nm, respectively. This corresponds to a Stokes shift of 8097 cm^{-1} and molar extinction coefficient of 19562 $M^{-1}cm^{-1}$. These results indicate that the compound does not exhibit a significant bathochromic shift compared to its phenanthrene analogs reported in literature. When tested in DSSCs, 7*H*-acenaphtho[1,2-*d*]imidazole achieved a power conversion efficiency of 0.22 % with Voc, Jsc and FF values 0.45 V, 0.78 mA/cm2 and 0.62, respectively.

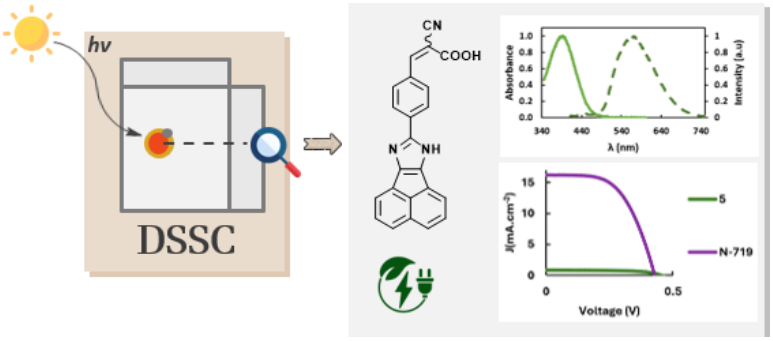

Keywords: Dye-sensitized solar cells, acenaphthylene-imidazole dyes, acenaphthoquinone, metal-free organic sensitizers

Introduction

Perovskite, polymer heterojunction, and dye-sensitized solar cells (DSSCs) comprise the three main categories of organic material-based solar cells, with DSSCs offering the distinct advantage of highly simplified processing. Although DSSCs have not reached the high efficiencies observed with perovskite solar cells (29.1%),[1] their power conversion efficiency (PCE) has steadily increased to ~14%.[2] Their inexpensive cost, manufacturing methods, roll-to-roll compatibility, easy processing capabilities on flexible substrates and outstanding efficiency in low-intensity or diffuse light,[3] position them as a viable alternative to conventional photovoltaic technologies,[4] particularly for indoor spaces[5,6] and smart window integration applications.[7]

Over the past three decades, significant effort has been devoted to designing highly efficient dyes for dye-sensitized solar cells (DSSCs). They can be divided into several classes, such as ruthenium-based dyes,[8] natural sensitizers,[9,10] and organic metal-free dyes.[11] Given the limited availability and high cost of raw materials in the first two cases, as well as the low efficiencies, current research efforts are directed toward metal-free organic sensitizers. These compounds offer several advantages, including enhanced chemical stability over long-term operation, high molar absorption coefficients, broad structural tunability, and simpler as well as more cost-effective synthetic routes compared with ruthenium-based alternatives.[11] Generally, these metal-free organic dyes for DSSC rely on small-molecule photosensitizers adsorbed on the surface of a mesoporous semiconducting material, typically TiO_2, and having a design based on a D-π-A architecture, where D is the donor, π is the π-bridge, and A is the acceptor. In donor–π–acceptor (D–π–A) sensitizers, the highest occupied molecular orbital (HOMO) is typically distributed over the electron-donating unit and the conjugated π-linker, whereas the lowest unoccupied molecular orbital (LUMO) is mainly concentrated on the electron-accepting segment.[12] Upon light absorption, this donor–acceptor arrangement promotes intramolecular charge transfer (ICT) from the donor toward the acceptor through the π-conjugated bridge. Furthermore, adjusting the chemical nature of the donor group and/or the π-spacer provides an effective strategy to tune the electronic energy levels, photophysical behavior, and photovoltaic efficiency of the dye. Although substantial progress has been made in the development of these devices, their power conversion efficiencies still lag behind those of other competing photovoltaic technologies. Therefore, further enhancement of DSSC performance requires the optimization of all major cell components, including the photoanode, sensitizing dye, electrolyte, counter electrode, and even the overall device architecture.[13] Hundreds of aromatic scaffolds for the dye counterpart have been the basis of extensive studies over the years. Donors typically consist of electron-rich aromatic amines or nitrogen heterocycles, including triarylamines,[14,15] carbazoles,[2] indolines,[16] or phenothiazines,[17] while acceptors are composed by electron-deficient moieties as a result of the need to have a group capable of binding to the TiO_2 surface, such as carboxylate, cyanoacrylate, catechol, sulfonate or trialkoxysilyl.[18] The π-bridges are a considerably more versatile molecular moiety, encompassing several sequential or fused polycyclic aromatic systems composed of combinations of benzene, thiophene, furan, indenyl and various other subunits. These extended π-conjugated systems often adopt planar arrangements which are valuable to electron transfer and absorption properties but often lead to formation of inactive dye aggregates on the semiconductor surface, an issue that can be mitigated with the inclusion of large alkyl or alkoxy groups.[19]

Acenaphthylene is a polycyclic aromatic hydrocarbon (PAH) consisting of a naphthalene unit in which positions 1 and 8 are linked by an ethylene bridge.[20] This critical building block has proven to be especially significant in the design and synthesis of organic electronic materials for various applications.[21] Figure 1 depicts several sensitizers used in DSSCs that are based on bis(triphenylamine)-fluoranthene,[22] acenaphthopyrazine,[23] and acenaphthoBODIPY,[24] scaffolds. Their performances range from 1.82 % to 4.57 %.

 ©AUTHOR(S)

π-Fused acenaphthylene-imidazole structure as *7H*-acenaphtho[1,2-*d*]imidazoles are also interesting organic molecules exhibiting excited-state intramolecular proton transfer (ESIPT).[25] The Debus–Radziszewski multicomponent reaction represents an efficient synthetic route for the construction of imidazole rings, typically involving the condensation of a 1,2-diketone with an aldehyde in the presence of an ammonia source. When an aniline derivative is introduced into this reaction system, the process affords a 1,2,4,5-tetrasubstituted imidazole scaffold.[26]

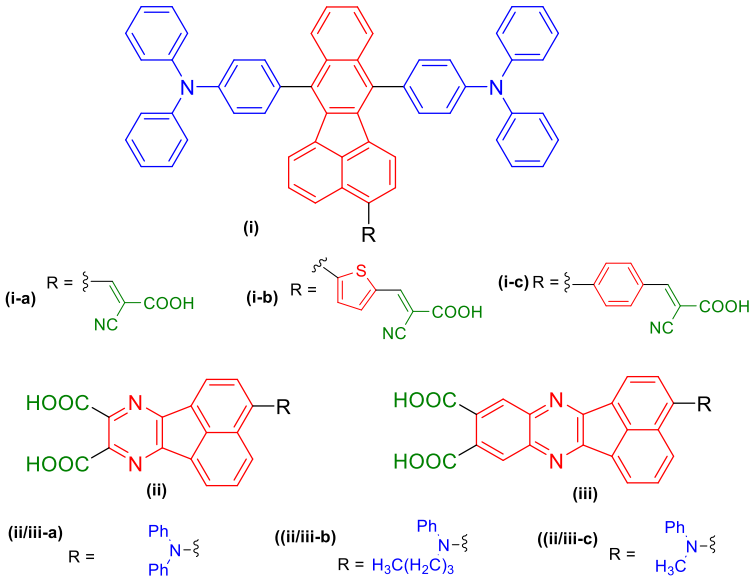

Figure 1. Structures of dyes incorporating bis(triphenylamine)-fluoranthene and acenaphthopyrazine cores.

When acenaphthoquinone is used as the 1,2-diketone counterpart in these reactions, it allows the synthesis of 7H-acenaphtho[1,2-d]imidazole derivatives (Scheme 1). Several catalysts such as Lewis acids (InF_3, ZnO),[27,28] silver salts (Ag_2CO_3),[29] ionic liquids (piperidinium hydrogen sulfate),[30] and other such as TiO_2,[31] I_2,[32] Ph_3CCl,[33] and L-proline,[34] can be employed to achieve the acenaphthylene-imidazole structures.

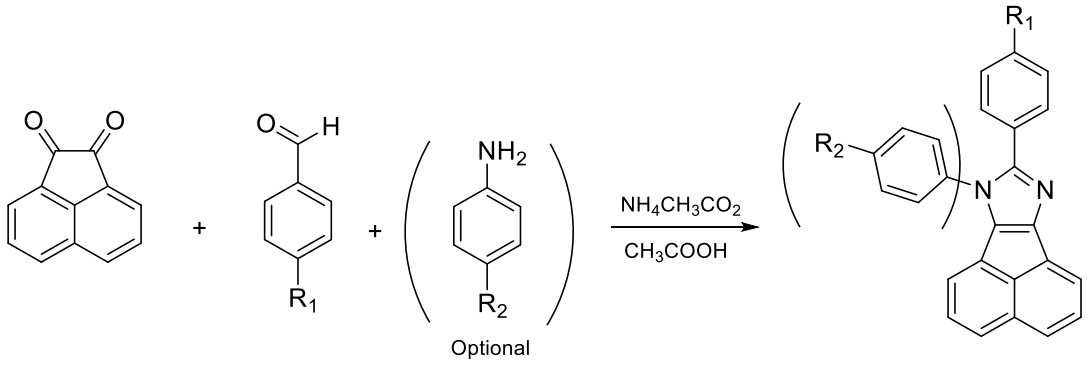

Scheme 1. Debus-Radziszewski reaction for the synthesis of 2,4,5-trisubstituted imidazole and 1,2,4,5-tetrasubstituted imidazole.[35]

Recently, Ramanujam et al.[36] reported the preparation of imidazole-based derivatives incorporating a fused phenanthrene framework which exhibited promising performance as sensitizers. Structural tuning

 ©**AUTHOR(S)**

through the incorporation of an anisole unit as an ancillary donor at the pyrrolic nitrogen led to an improvement in power conversion efficiency from 5.26 % to 6.71% with 7.62% for the N719 reference dye. The compounds were easily synthesized by reacting 9,10-phenanthrenequinone, terephthaladehyde, *p*-anisidine, and ammonium acetate in glacial acetic acid under reflux.

Although some examples have been reported where the acenaphthylene core is present in some dye sensitizers (Scheme 1), those reporting 7H-acenaphtho[1,2-d]imidazole units in this field remain to be explored. Taking this into account, a family based on 7H-acenaphtho[1,2-d]imidazole was intent to be prepared for the first time.

Results and Discussion

Synthesis. The synthesis of the 7H-acenaphtho[1,2-*d*]imidazole dye was attained using the method reported by Singh *et al*.[35] by reacting the acenaphthoquinone (**1**), with terephthalaldehyde (**2**) and ammonium acetate as the nitrogen source, in glacial acetic acid under reflux. The 4-(7*H*-acenaphtho[1,2-*d*]imidazol-8-yl)benzaldehyde (**3**) was obtained in low yield (12.9 %). The formation of the oxazole analogue (**4**) was also observed (η = 5.1 %). Crucial for the identification without doubt was the difference observed in the LC-ESIMS spectra of one Dalton between the two compounds due to the appearance of the molecular ion peaks at *m*/*z* 297.1 for **3** and at *m*/*z* 298.1 for **4**. It was also observed that in the ^{1}H NMR spectrum of **4** the signals are downfield than those of **3** due to the deshielding effect that the oxygen atom causes.[37] Both compounds could be isolated by preparative TLC. The possibility of formation of these two species was reported previously.[38] Specifically, it has been reported that at low temperatures oxazole products are formed whereas, at high temperatures only the imidazole or a mixture with oxazole is obtained.[38]

The cyanoacrylic acid moiety was incorporated into imidazole derivative **3** through a Knoevenagel reaction employing cyano acetic acid, ammonium acetate, and glacial acetic acid.[36] This transformation afforded the target chromophore 5 in 70.1% yield (Scheme 2). Any attempt to prepare the thiophene analogues (**6**) with thiophene derivatives (**7a-b**) only afforded complex mixtures. Also, any attempts to introduce an electron-donating group in the pyrrolic nitrogen were unsuccessful. Although reported elsewhere,[39] any attempts that we underwent to introduce aniline and *p*-anisidine onto the imidazole core led to the formation of the corresponding subproducts *N*-phenylacetamide and *N*-(4-methoxyphenyl)acetamide. These species arise from the acetylation of the anilines by acetic acid. In some cases, the extent of this side reaction exceeded 50% conversion, thereby significantly hindering the efficiency of the desired functionalization. Alternative methods, as those reported in literature that rely on the use of L-proline as a catalyst[34] or employ ethanol as solvent,[40] were also evaluated. These included performing the reactions in sealed tubes under elevated pressure and temperature to promote the coupling between the intermediates. These methods only led to the consumption of the starting materials, but no evidence of the formation of the N-substituted 7*H*-acenaphtho[1,2-*d*]imidazol-8-yl derivatives was observed. Instead, intermediates were obtained, namely the corresponding Schiff bases of **2**. Except for compound 5, all efforts to obtain additional 2,4,5-trisubstituted and 1,2,4,5-tetrasubstituted imidazoles were unsuccessful, either due to the formation of side products or the low reactivity of the intermediates. As a result, only compound 5 was further evaluated in DSSC devices.

 ©**AUTHOR(S)**

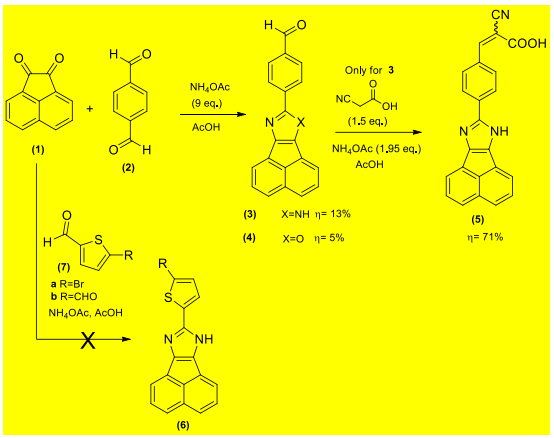

Scheme 2. Synthesis of the 7*H*-acenaphtho[1,2-*d*]imidazol-8-yl derivative (**5**).

Photophysical and photovoltaic studies

The absorption and emission spectra of compound **5** were measured in methanol (Figure 2). The compound exhibits an absorption maximum at 390 nm with a molar extinction coefficient of 19562 $M^{-1}cm^{-1}$. Compared with similar compounds with a phenanthrene core reported by Ramanujam et al.,[36] compound **5** presents its absorption band at shorter wavelengths, the literature analogues exhibit two bands at longer wavelengths (426 nm and 450 nm) with a lower molar extinction coefficient (17500 M^{-1} cm^{-1}). Additionally, compound **5** has an emission maximum at 570 nm, corresponding to a Stokes shift of 8097 cm^{-1}. The efficiency of compound **5** was tested in DSSC devices, and the current-voltage (*I-V*) curve was measured. The photovoltaic parameters — open-circuit voltage (V_{oc}), short-circuit current (J_{sc}), fill factor (FF), and photovoltaic conversion efficiency (η), together with the *I-V* curve are displayed in Figure 3 and Table 1, respectively. The compound presented V_{oc}, values that are comparable and even slightly better than the reference N-719. Unfortunately, under comparable cell setup and assembly the photocurrent values, J_{sc}, are very low 0.78 mA/cm^2, leading to an overall low efficiency of 0.22 %. The low value for J_{sc} cannot be ascribed to the ability to absorb photons, since the extinction coefficient compares well with N-719 (ca. 14000 $M^{-1}cm^{-1}$). The low photocurrent can be related to the efficiency of dye loading and the aggregation quenching of the excited states due to the planarity of the compound, prone to undergo $\pi\pi$ stacking interactions. The photophysical parameters of compound 5, particularly the VOC and the molar absorption coefficient, are promising. Adjustment of the dye-loading and cell assembly conditions could possibly lead to Jsc values of compound 5 comparable to that of N-719.

 ©AUTHOR(S)

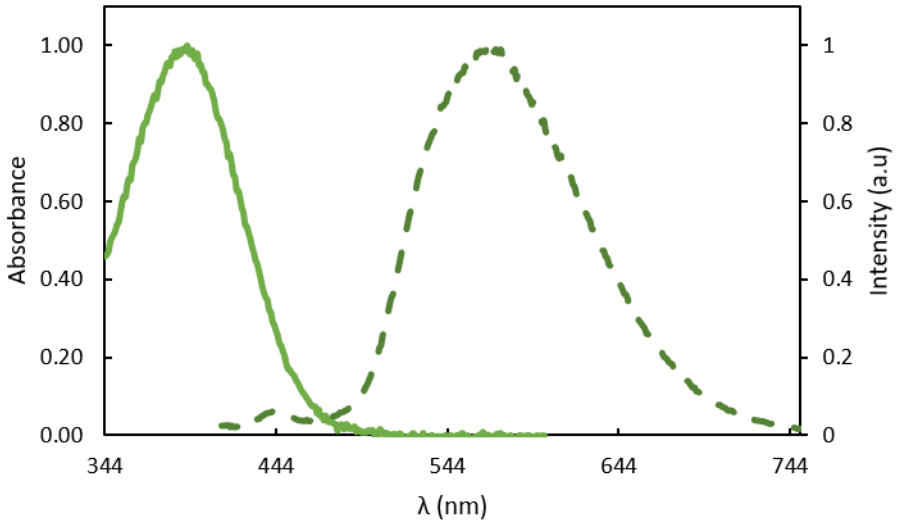

Figure 2. Normalized absorption (solid line) and fluorescence emission (dotted line; λ_{exc}=390 nm) spectra of compound **5** in methanol at room temperature.

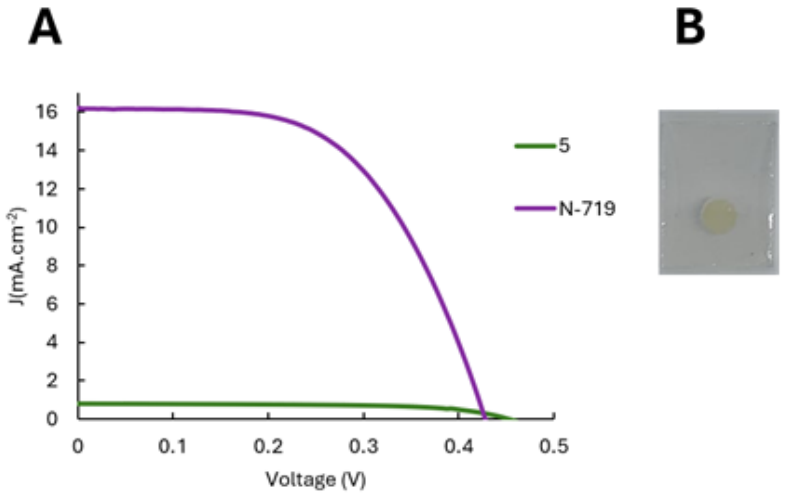

Figure 3. A: Current–voltage (*I*–V) curves of the test cells based on dye **5** and the reference N-719 under simulated AM 1.5G (100 mW.cm^{-2}) illumination, showing the best performing cell. B: Dye absorption of compound **5** on a TiO_2 anode.

Table 1. Performance values of the test cells based on the synthesized dyes and reference dye N-719 under 100 mW.cm^{-2} AM 1.5G illumination. Reported values correspond to the average of at least two independently assembled cells per dye, each measured five times. Photoanodes were prepared by immersion in a 0.5 mM ethanolic dye solution for 16 h at room temperature in the dark. The electrolyte composition: 0.8 M LiI and 0.05 M I_2 in acetonitrile/valeronitrile (85:15, % v/v).

Dye	V_{oc} (V)	J_{sc} (mA/cm^2)	J_{max} (mA/cm^2)	V_{max} (V)	FF	η (%)
5	0.450	0.78	0.64	0.346	0.62	0.22
N-719	0.422	16.33	13.51	0.277	0.54	3.75

©**AUTHOR(S)**

Conclusions

A 7*H*-acenaphtho[1,2-d]imidazole derivative, namely 3-(4-(7*H*-acenaphtho[1,2-d]imidazol-8-yl)phenyl)-2-cyanoacrylic acid (**5**) was successfully synthesized, featuring a phenyl unit as a π-bridge and cyanoacrylic acid as the anchoring group. The photovoltaic performance of this dye was evaluated, and although the relatively low efficiency (η = 0.22 %) the V_{oc} and FF values were higher than those of the reference dye N-719. In contrast, attempts to prepare the corresponding thiophene analogue were unsuccessful. Similarly, the synthesis of 1,2,4,5-tetrasubstituted imidazole derivatives could not be achieved due to the formation of side products as a result of the low reactivity of the intermediates.

Experimental Section

General. Commercially available solvents and reagents (Merck KGaA, Darmstadt, Germany) were used without additional purification. Solvent drying was accomplished by using M2A molecular sieves (Merck KGaA), according to the standard published methodologies.[41] Thin-layer chromatography (TLC) was carried out utilizing aluminum-backed Kieselgel 60 F254 silica gel plates (Merck KGaA), with detection achieved under UV illumination at 254 and 336 nm. Preparative-layer chromatography (PLC) was executed on Keiselgel 60 F254 silica gel plates (Merck KGaA). For normal phase column chromatography, Kieselgel 60A (Carlo Erba) with particle size range of 40-63 µm was employed.[42] A Bruker Avance III 400 spectrometer (Billerica, MA, USA) was used to collect ^{1}H (400 MHz) and ^{13}C (101 MHz) NMR spectra. High-resolution mass spectrometry (HRMS) was performed at University of Salamanca (NUCLEUS research support service) on a Thermo Orbitrap QExactive Focus mass spectrometer line coupled to a Thermo Vanquish core HPLC with a diode array UV detector. Optical absorption profiles were captured via a VWR M4 spectrometer (Ismaning, Germany). Lastly, fluorescence spectra were generated on a SPEX Fluorolog 1681 0.22 m spectrofluorimeter (Metuchen, NJ, USA) with a 150 W Xe−Hg lamp, followed by automated wavelength response corrections.

DSSCs fabrication and photovoltaic characterization. Following a previously reported methodology,[43] conductive fluorine-doped tin oxide (FTO) glass substrates (TEC7, Greatcell Solar) were first cleansed with detergent and sequentially rinsed with water and ethanol. For anode preparation, the cleaned FTO plates were treated with a 40 mM aqueous $TiCl_4$ solution (40 mM) at 70 °C for 30 min. After a final rinse with water and ethanol, the substrates were sintered at 500 °C for 30 min. This procedure establishes a compact 'blocking layer' that suppresses charge recombination at the FTO interface while simultaneously optimizing the adhesion of later nanocrystalline deposits. Subsequently, transparent TiO_2 films were deposited onto the pre-treated plates through the screen-printing technique, utilizing a commercial titania paste with 43.80 mesh per cm^2 polyester fiber frame (18NR-T, GreatcellSolar, Queanbeyan, Australia). After an initial drying step of the coated plates at 125 °C on a hotplate, a second layer was deposited and dried in the same way. The final sintering process was achieved through a stepped thermal profile, where the temperature was progressively ramped to 325 °C, increased to 375 °C over 5 min, and finally brought to 500 °C. The plates were maintained at this temperature for 30 min at this temperature and subsequently cooled to room temperature, followed by a second treatment with $TiCl_4$/water solution (40 mM) in the previously reported conditions. The fabrication of the anodes was completed by screen-printing deposition of reflective titania paste (WER2-O, Greatcell Solar)

 ©**AUTHOR(S)**

and sintering at 500 °C. This layer features 150-200 nm anatase particles to optimize the photocurrent. The plates were then cut into rectangles (size: 2 cm × 1.5 cm), each displaying an active area of 0.196 cm^2 and a thickness of 15 µm. These were immersed overnight in a 0.5 mM dye solution prepared in CH_2Cl_2:MeOH:H_2O (65:35:5, %v/v), at room temperature protected from the light. The photoanodes were rinsed with the same solvent to remove the excess dye.

Cathodes were fabricated from 2 cm × 2 cm FTO-glass plates, each with a 1.0 mm diameter hole. To eliminate organic residues and residual glass powder, the substrates were thoroughly washed with water and ethanol. A transparent Pt catalyst layer (PT1, Greatcell Solar) was applied to the conductive surface via the doctor blade method. Film thickness and an uncoated 0.5 cm electrical contact margin were defined using a 3M Magic adhesive tape spacer. A glass rod was swept over the tape to distribute the Pt paste evenly. Following tape removal, the resulting cathodes were heated at 550 °C for 30 min. Finally, the devices were assembled into a sandwich architecture by hot-pressing the photoanode and cathode together, using a Surlyn ionomer film (Meltonix 1170-25, Solaronix SA) as the sealant.

The liquid electrolyte consisted of an I^-/I_3^- redox pair (0.8 M LiI and 0.05 M I_2) dissolved in a mixture of acetonitrile and valeronitrile (85:15, % v/v). This solution was injected into the assembled device through the pre-drilled hole by using a vacuum back-filling technique, after which the orifice was sealed with adhesive tape. To ensure reproducibility, a minimum of two identical cells were fabricated for each dye, and the efficiencies were measured 5 times for each device.

The device performance was evaluated via photocurrent-voltage measurements acquired with Keithley SourceMeter multimeter. To replicate solar irradiation, an Oriel solar simulator (Model LCS-100 Small Area Sol1A, 300 W Xe Arc lamp equipped with AM 1.5G filter, 100 mW cm^{-2}) was employed.

Synthesis of 7*H*-acenaphtho[1,2-*d*]imidazole derivatives

Synthesis of 4-(7*H*-acenaphtho[1,2-*d*]imidazol-8-yl)benzaldehyde (3). A mixture of terephthalaldehyde (**2**) (100.6 mg, 0.75 mmol, 1 eq.), acenaphthoquinone (**1**) (134.45 mg, 0.74 mmol), ammonium acetate (544.1 mg, 7.1 mmol, 9.5 eq.) in glacial acetic acid (3.4 mL) was refluxed for 1 hour. The reaction was followed by TLC using the eluent hexane: EtOAc 6:4. Then it was cooled to room temperature and the quenching was performed by adding H_2O. The formed solid was filtered and washed with H_2O via centrifugation. The resulting solid was purified by flash column chromatography using as eluent CH_2Cl_2 to CH_2Cl_2/5 % MeOH. It was possible to isolate a red solid corresponding to the secondary product 4-(acenaphtho[1,2-d]oxazol-8-yl)benzaldehyde (**4**) (11.4 mg, 0.038 mmol, η = 5.1 %). The fraction containing the desired product was purified a second time by preparative chromatography using the eluent CH_2Cl_2/2.5% MeOH, it was possible to obtain 28.3 mg of an orange solid corresponding to 4-(7*H*-acenaphtho[1,2-*d*]imidazol-8-yl)benzaldehyde (**3**) (0.096 mmol, η = 12.9%). Although NMR data have been reported in the literature,[35] direct comparison is difficult because different solvents were used for the measurements. ^{1}H NMR (500 MHz, $CDCl_3$) δ (ppm): 9.66 (s, 1H, CHO), 7.88 (d, *J* 8.0 Hz, 2H, ArH), 7.62 (d, *J* 8.0 Hz, 4H, ArH), 7.59 (d, *J* 8.0 Hz, 2H, ArH), 7.43 (t, *J* 7.8 Hz, 2H, ArH). LC-ESI-MS, RT: 8.12 min, *m/z:* 297.1 $[M+H]^+$ 4-(Acenaphtho[1,2-d]oxazol-8-yl)benzaldehyde (**4**): ^{1}H NMR (500 MHz,$CDCl_3$) δ (ppm): 10.08 (s, 1H, CHO), 8.34 (d, *J* 8.5 Hz, 2H, ArH), 8.01 (d, *J* 8.5 Hz, 2H, ArH), 7.95 (d, *J* 6.5 Hz, 1H, ArH), 7.87 – 7.81 (m, 3H, ArH), 7.61 (ddd, *J* 8.3, 7.0, 2.5 Hz, 2H, ArH). LC-ESI-MS, RT: 20.16 min, *m/z*: 298.1 $[M+H]^+$.

Synthesis of 3-(4-(7*H*-acenaphtho[1,2-*d*]imidazol-8-yl)phenyl)-2-cyanoacrylic acid (5). Following the procedure described by Sivanadanam[36] a mixture of 4-(7*H*-acenaphtho[1,2-*d*]imidazol-8-yl)benzaldehyde (**3**) (21.3 mg, 0.07 mmol), cyanoacetic acid (9.1 mg, 0.11mmol,1.5 eq.), ammonium acetate (10.7 mg, 0.14 mmol, 1-9.5 eq.) in 3.6 mL of glacial acid acetic was stirred at 85°C under N_2 atmosphere for 20 hours. The

 ©**AUTHOR(S)**

consumption of aldehyde was monitored by TCL using the eluent CH_2Cl_2 / MeOH 2.5 %. Then the reactional mixture was cooled to room temperature, and the quenching was performed by adding cold water. An aqueous solution of $NaHCO_3$ was added, and the solid was centrifuged and washed with water. It was possible to afford 18.3 mg of an orange solid corresponding to 3-(4-(7*H*-acenaphtho[1,2-*d*]imidazol-8-yl)phenyl)-2-cyanoacrylic acid (**5**) (0.05 mmol, η = 70.1 %). ATR (v (cm^{-1})): 3388 (m, O-H), 3054 (w, C-Har), 2218 (w, CΞN), 1624 (m, C=O), 1560 (s, C=N). ^{1}H NMR (500 MHz, DMSO-d_6) δ (ppm): 13.58 (br s, 1H), 8.30 (br s, 1H, CH_2), 8.23 – 8.09 (m, 4H, ArH), 7.79 (br s, 4H, ArH), 7.59 (br s, 2H, ArH). ESI-MS (+) *m/z*: 364.1 $[M+H]^+$. ESI-HRMS calculated for $C_{23}H_{14}N_3O_2$, 364.1086; Found: 364.1074 $[M+H]^+$.

Acknowledgements

This work received support and help from FCT/MCTES (LA/P/0008/2020 DOI 10.54499/LA/P/0008/2020, UIDP/50006/2020 DOI 10.54499/UIDP/50006/2020 and UIDB/50006/2020 DOI 10.54499/UIDB/50006/2020), through national funds and project PTDC/QUI-QOR/7450/2020 "Organic Redox Mediators For Energy Conversion" through Fundação para a Ciência e a Tecnologia I. P.-FCT. FCT/MCTES is also acknowledged for the National NMR Facility (RECI/BBB-BQB/0230/2012 and RECI/BBB-BEP/0124/2012,) and Ph.D. grant https://doi.org/10.54499/SFRH/BD/145324/2019 (G.M.).

Supplementary Material

General procedures, experimental details, characterization data, NMR and IR spectra are given in the supplementary material file associated with this manuscript.

References

1. Liu, Z.; Lin, R.; Wei, M.; Yin, M.; Wu, P.; Li, M.; Li, L.; Wang, Y.; Chen, G.; Carnevali, V.; Agosta, L.; Slama, V.; Lempesis, N.; Wang, Z.; Wang, M.; Deng, Y.; Luo, H.; Gao, H.; Rothlisberger, U.; Zakeeruddin, S. M.; Luo, X.; Liu, Y.; Grätzel, M.; Tan, H. *Nat. Mater.* **2025**, *24*, 252. DOI:10.1038/s41563-024-02073-x.
2. Kakiage, K.; Aoyama, Y.; Yano, T.; Oya, K.; Fujisawa, J.; Hanaya, M. *Chem. Commun.* **2015**, *51*, 15894. DOI:10.1039/C5CC06759F.
3. Gong, J.; Liang, J.; Sumathy, K. *Renew. Sustain. Energy Rev.* **2012**, *16*, 5848. DOI:10.1016/j.rser.2012.04.044.
4. Muñoz-García, A. B.; Benesperi, I.; Boschloo, G.; Concepcion, J. J.; Delcamp, J. H.; Gibson, E. A.; Meyer, G. J.; Pavone, M.; Pettersson, H.; Hagfeldt, A.; Freitag, M. *Chem. Soc. Rev.* **2021**, *50*, 12450. DOI:10.1039/D0CS01336F.
5. Devadiga, D.; Selvakumar, M.; Shetty, P.; Santosh, M. S. *J. Electron. Mater.* **2021**, *50*, 3187. DOI:10.1007/s11664-021-08854-3.
6. Aslam, A.; Mehmood, U.; Arshad, M. H.; Ishfaq, A.; Zaheer, J.; Ul Haq Khan, A.; Sufyan, M. *Solar Energy* **2020**, *207*, 874. DOI:10.1016/j.solener.2020.07.029.
7. Kim, J.-H.; Han, S.-H. *Sustainability* **2020**, *12*, 8961. DOI:10.3390/su12218961.
8. Vougioukalakis, G. C.; Philippopoulos, A. I.; Stergiopoulos, T.; Falaras, P. *Coord. Chem. Rev.* **2011**, *255*, 2602. DOI:10.1016/j.ccr.2010.11.006.

 ©**AUTHOR(S)**

9. Syafinar, R.; Gomesh, N.; Irwanto, M.; Fareq, M.; Irwan, Y. M. *Energy Procedia* **2015**, *79*, 896. DOI:10.1016/j.egypro.2015.11.584.
10. Amogne, N. Y.; Ayele, D. W.; Tsigie, Y. A. *Mater. Renew. Sustain. Energy* **2020**, *9*, 23. DOI:10.1007/s40243-020-00183-5.
11. Shalini, S.; Balasundaraprabhu, R.; Kumar, T. S.; Prabavathy, N.; Senthilarasu, S.; Prasanna, S. *Int. J. Energy Res.* **2016**, *40*, 1303. DOI:10.1002/er.3538.
12. Ji, J.-M.; Zhou, H.; Kim, H. K. *J. Mater. Chem. A* **2018**, *6*, 14518. DOI:10.1039/C8TA02281J.
13. Ye, M.; Wen, X.; Wang, M.; Iocozzia, J.; Zhang, N.; Lin, C.; Lin, Z. *Materials Today* **2015**, *18*, 155. DOI:10.1016/j.mattod.2014.09.001.
14. Yahya, M.; Bouziani, A.; Ocak, C.; Seferoğlu, Z.; Sillanpää, M. *Dyes Pigm.* **2021**, *192*, 109227. DOI:10.1016/j.dyepig.2021.109227.
15. Mahmood, A. *Solar Energy* **2016**, *123*, 127. DOI:10.1016/j.solener.2015.11.015.
16. Yang, J.; Ganesan, P.; Teuscher, J.; Moehl, T.; Kim, Y. J.; Yi, C.; Comte, P.; Pei, K.; Holcombe, T. W.; Nazeeruddin, M. K.; Hua, J.; Zakeeruddin, S. M.; Tian, H.; Grätzel, M. *J. Am. Chem. Soc.* **2014**, *136*, 5722. DOI:10.1021/ja500280r.
17. Lin, R. Y.; Wu, F.; Li, C.; Chen, P.; Ho, K.; Lin, J. T. *ChemSusChem* **2015**, *8*, 2503. DOI:10.1002/cssc.201500589.
18. Zhang, L.; Cole, J. M. *ACS Appl. Mater. Interfaces* **2015**, *7*, 3427. DOI:10.1021/am507334m.
19. Do, K.; Kim, D.; Cho, N.; Paek, S.; Song, K.; Ko, J. *Org. Lett.* **2012**, *14*, 222. DOI:10.1021/ol203012s.
20. Sahoo, B. M.; Ravi Kumar, B. V. V.; Banik, B. K.; Borah, P. *Curr. Org. Synth.* **2020**, *17*, 625. DOI:10.2174/1570179417666200713182441.
21. Liu, Y.-H.; Perepichka, D. F. *J. Mater. Chem. C* **2021**, *9*, 12448. DOI:10.1039/D1TC02826J.
22. Wang, T.; Han, J.; Zhang, Z.; Xu, B.; Huang, J.; Su, J. *Tetrahedron* **2012**, *68*, 10372. DOI:10.1016/j.tet.2012.09.013.
23. Kong, Z.; Zhou, H.; Cui, J.; Ma, T.; Yang, X.; Sun, L. *J. Photochem. Photobiol. A: Chem.* **2010**, *213*, 152. DOI:10.1016/j.jphotochem.2010.05.017.
24. Okujima, T.; Shida, Y.; Ohara, K.; Tomimori, Y.; Nishioka, M.; Mori, S.; Nakae, T.; Uno, H. *J. Porphyr. Phthalocyanines* **2014**, *18*, 752. DOI:10.1142/S1088424614500503.
25. Somasundaram, S.; Kamaraj, E.; Hwang, S. J.; Jung, S.; Choi, M. G.; Park, S. *J. Mol. Struct.* **2017**, *1137*, 43. DOI:10.1016/j.molstruc.2017.02.025.
26. Saxer, S.; Marestin, C.; Mercier, R.; Dupuy, J. *Polym. Chem.* **2018**, *9*, 1927. DOI:10.1039/C8PY00173A.
27. Jayabharathi, J.; Thanikachalam, V.; Ramanathan, P.; Arunpandiyan, A. *Spectrochim. Acta A Mol. Biomol. Spectrosc.* **2014**, *121*, 551. DOI:10.1016/j.saa.2013.10.097.
28. Bahrami, K.; Khodaei, M. M.; Nejati, A. *Monatsh. Chem.* **2011**, *142*, 159. DOI:10.1007/s00706-010-0428-8.
29. Sarkar, R.; Mukhopadhyay, C. *Eur. J. Org. Chem.* **2015**, *2015*, 1246. DOI:10.1002/ejoc.201403465.
30. Albayati, M. R.; Marzouk, Adel. A.; Abdelhamid, A. A. *J. Heterocycl. Chem.* **2019**, *56*, 1514. DOI:10.1002/jhet.3525.
31. Jayabharathi, J.; Ramanathan, P.; Thanikachalam, V. *New J. Chem.* **2015**, *39*, 142. DOI:10.1039/C4NJ01515K.
32. Okda, H. E.; El Sayed, S.; Otri, I.; Ferreira, R. C. M.; Costa, S. P. G.; Raposo, M. M. M.; Martínez-Máñez, R.; Sancenón, F. *Dyes Pigm.* **2019**, *162*, 303. DOI:10.1016/j.dyepig.2018.10.017.
33. Moosavi-Zare, A. R.; Asgari, Z.; Zare, A.; Zolfigol, M. A.; Shekouhy, M. *RSC Adv.* **2014**, *4*, 60636. DOI:10.1039/C4RA10589C.
34. Sarkar, R.; Chaudhuri, T.; Karmakar, A.; Mukhopadhyay, C. *Org. Biomol. Chem.* **2015**, *13*, 11674. DOI:10.1039/C5OB01646K.
35. Singh, I.; Rani, R.; Luxami, V.; Paul, K. *Eur. J. Med. Chem.* **2019**, *166*, 267. DOI:10.1016/j.ejmech.2019.01.053.
36. Sivanadanam, J.; Aidhen, I. S.; Ramanujam, K. *New J. Chem.* **2020**, *44*, 10207. DOI:10.1039/D0NJ00137F.

 ©AUTHOR(S)

37. Malta, G. New mono- and hetero-branched sensitizers for DSSC, NOVA University of Lisbon: Portugal, 2024. http://hdl.handle.net/10362/180129.
38. El'chaninov, M. M.; Achkasova, A. A.; El'chaninov, I. M. *Russ. J. Gen. Chem*. **2014**, *84*, 1697. DOI:10.1134/S1070363214090096.
39. Yu, R.; Kan, W.; Qi, X.; Zhang, Y.; Ding, L.; Wang, L.; Zhao, B. *SSRN* **2023**. DOI:10.2139/ssrn.4511188.
40. Thanikachalam, V.; Sarojpurani, E.; Jayabharathi, J.; Jeeva, P. *New J. Chem.* **2017**, *41*, 2443. DOI:10.1039/C6NJ03801H.
41. Williams, D. B. G.; Lawton, M. *J. Org. Chem.* **2010**, *75*, 8351. DOI:10.1021/jo101589h.
42. Still, W. C.; Kahn, M.; Mitra, A. *J. Org. Chem.* **1978**, *43*, 2923. DOI:10.1021/jo00408a041.
43. Malta, G.; Pina, J.; Lima, J. C.; Parola, A. J.; Branco, P. S. *ACS Omega* **2024**, *9*, 14627. DOI:10.1021/acsomega.4c01201.

This paper is an open access article distributed under the terms of the Creative Commons Attribution (CC BY) license (http://creativecommons.org/licenses/by/4.0/)